Journal of Physics: Conference Series **119** (2008) 032019 doi:10.1088/1742-6596/119/3/032019

Track-based alignment of the ATLAS Inner Detector

Gonzalez-Sevilla, S.
On behalf of the ATLAS Collaboration

Instituto de Física Corpuscular (IFIC), University of València/CSIC, Spain

E-mail: segonzal@ific.uv.es

Abstract. ATLAS is a general purpose experiment currently under final assembly for the Large Hadron Collider at CERN. The Inner Detector is the ATLAS internal tracker. It comprises different complementary technologies for tracking purposes: silicon and straw tubes gaseous detectors. In order to reach the optimal performance of the tracker, a high-precision alignment of the huge number of detecting elements is required. Several track-based alignment algorithms have been developed for the Inner Detector. An extensive validation has been performed with simulated events and real data coming from the ATLAS Combined Testbeam and data-taking of cosmic rays on surface. This paper reports on the principle of the different methods, computing requirements and results obtained with real data. Finally, preliminary results from the ATLAS Computing System Commissioning and Calibration Data Challenge are shown.

1. Introduction

The ATLAS detector [1] is a general-purpose experiment actually being assembled at CERN for the Large Hadron Collider (LHC). The LHC will provide proton-proton collisions with a center-of-mass energy of 14 TeV, a frequency of 40 MHz and a nominal luminosity of $10^{34}\,cm^{-2}s^{-1}$.

The Inner Detector (ID) [2] is the ATLAS internal tracker. It combines high-resolution discrete silicon (pixel and microstrip) detectors in the innermost layers with a continuous gaseous straw-tube detector in the outermost radii. This layout ensures a robust pattern recognition, momentum and charge determination, precise vertex measurements, electron identification and pion separation. The three different sub-systems are from the inside-out (see figure 1): the Pixel detector, the Semiconductor Tracker (SCT) and the Transition Radiation Tracker (TRT). The ID geometry is cylindrical, with a length of $\sim$ 6.2 m and a diameter of $\sim$ 2.5 m. A central superconducting solenoid surrounding the TRT provides a 2 T axial field.

The Pixel detector consists of a barrel region with three cylindrical layers and two symmetric end-caps each containing three disks for tracking in the forward region. All pixel modules are identical, with a sensor segmented in $50\,\mu m \times 400\,\mu m$ pixels providing a 2D readout with a binary resolution of $14\,\mu m \times 115\,\mu m$ in the azimuth ($r\phi$) and transverse planes (z) respectively.

The SCT is made of four layers in the barrel region and nine disks in each of the two end-caps. Different types of modules have been built for the SCT, all with the same components but differing only in their geometry. A module is composed of two pairs of single-sided silicon microstrip detectors glued back-to-back with a relative stereo angle of 40 mrad. The strip pitch is $80\,\mu m$ for the barrels and varying from $\sim 55\,\mu m$ to $\sim 90\,\mu m$ for end-cap modules due to their fan-out geometry. The single plane resolution in the direction perpendicular to the strips is $\sim 23\,\mu m$.

© 2008 IOP Publishing Ltd

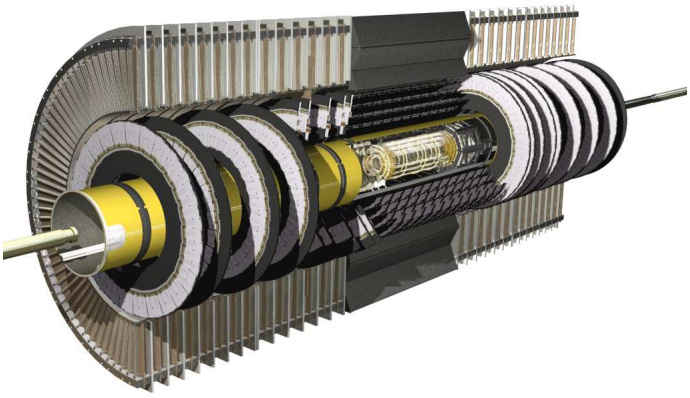

Figure 1. View of the ATLAS Inner Detector.

The TRT consists in $\sim 3\times10^5$ straw tubes, arranged in 32 modules in each of the three barrel layers and 20 wheels in each of the two end-caps. The principle of operation is the measurement of the transition radiation from the passage of a charged particle through the straws. A gold-plated tungsten anode wire with a diameter of $30\,\mu m$ is located at the center of each straw of 2 mm radius, providing a single measurement resolution of $\sim 130\,\mu m$.

2. Inner Detector alignment requirements and strategy

High-precision electroweak measurements will be performed in ATLAS. As an example, the mass of the W-boson is aimed to be determined with a systematic error better than $15\,MeV/c^2$ providing a strong consistency test of the Standard Model and allowing to constrain the Higgs mass [3]. This requirement implies the knowledge of the absolute momentum scale to an accuracy of 0.02%. From the alignment point-of-view, the absolute position of the detecting devices must be known at the micron level in the $r\phi$ plane.

The strategy for the alignment of the Inner Detector is focussed on track-based offline alignment algorithms complemented by a Frequency Scanning Interferometric (FSI) system in the SCT barrels. The initial knowledge of the module positions is provided by optical and mechanical surveys during the assembly and installation stages.

3. Track-based alignment approaches

Several track-based alignment algorithms have been developed for the Inner Detector and are already implemented under the ATLAS software framework (Athena). All of them make use of the residual information, *i.e.*, the distance from the reconstructed track to the recorded hit.

The Robust approach [4] is intended for the alignment of the silicon tracker profitting from the fact that adjacent modules overlap. It makes use of both residual ($\bar{r}$) and overlap ($\bar{o}r$) residual measurements to compute in-plane corrections:

$$\mathrm{shift}_{\mathrm{X/Y}} = -\sum_{j=1}^{n} \frac{s_j}{(\delta s_j)^2} \Big/ \sum_{j=1}^{n} \frac{1}{(\delta s_j)^2} \qquad (n \leq 3) \tag{1}$$

where $s_1 = \bar{r}$, $s_2 = \sum \bar{o}r_\phi$ and $s_3 = \sum \bar{o}r_z$. The variables δs_j describe the uncertainties in these measurements. Additional factors controlling the relative weights of overlap and mean residuals, as well as the number of overlap and non-overlap hits, are also defined. In addition to the in-plane translations, corrections to systematic radial translations can also be computed.

The Global χ^2 approach [5, 6] is based on the minimization with respect to the alignment parameters of a χ^2 function defined as

$$\chi^2 = \sum_{tracks} r^T V^{-1} r \tag{2}$$

where $r(a, \pi)$ is the vector of hit residuals depending on both alignment (a) and track parameters (π), and V is the covariance matrix of the hit measurements including the contribution from Multiple Coulomb Scattering (MCS). After a linear expansion of the residuals around some initial estimates (a_0, π_0) and neglecting second order derivatives, the alignment corrections are given as

$$\delta a = -\left(\sum_{trks} \frac{\partial r^T}{\partial a_0} W \frac{\partial r}{\partial a_0}\right)^{-1} \left(\sum_{trks} \frac{\partial r^T}{\partial a_0} W r(\pi_0, a_0)\right) \equiv -M^{-1}\nu \tag{3}$$

where $W = V^{-1} - V^{-1}(E^T V^{-1} E)^{-1} E^T V^{-1}$ and $E \equiv \partial r / \partial \pi_0$. The matrix M is a symmetric $n \times n$ matrix, where n is the total number of alignment degrees of freedom (DoFs) of the system. The Global χ^2 approach takes into account six DoFs per module and the inter-module correlations, but does require the inversion of the very large matrix M. For the ATLAS silicon system (Pixel and SCT), $n \sim 35000$. Different methods to solve large systems of linear equations have been investigated in terms of time performance and accuracy. As an example, the diagonalization of a system representing the full Pixel detector (12500 DoFs) took only 15 seconds using a sparse symmetric technique (MA27) in a single Intel Xeon 3.0 GHz processor [7].

The Local χ^2 alignment algorithm [8, 9] shares the same principle as the Global χ^2 approach. In this case, the dependence of track parameters with respect to alignment parameters is removed by using unbiased residuals (the hit in the module being aligned is removed from the track fit) assuming the tracking uncertainty is smaller than the measurement error. Neglecting MCS, the full covariance matrix V is thus diagonal, containing only the measurements uncertainties. The Local χ^2 approach solves 6×6 matrices corresponding to the six DoFs per module. Therefore, for module i, the alignment corrections are given by:

$$\delta a_i = -\left(\sum_{tracks} \frac{\partial r_i^T}{\partial a} \frac{1}{\sigma_i^2} \frac{\partial r_i}{\partial a}\right)^{-1} \left(\sum_{tracks} \frac{1}{\sigma_i^2} \frac{\partial r_i^T}{\partial a} r_i\right) \tag{4}$$

The inter-module correlations are restored by performing a certain number of iterations, where track fits and the computation of alignment corrections are alternated in a iterative way.

Originally intended for the alignment of TRT modules only, TRTAlignAlg [10] has been extended for dealing with Pixel and SCT modules. This approach is also based on the minimization of a χ^2 for a large sample of tracks and implements both local and global principles. While using the local method, CLHEP [11] is used to invert the second derivative matrices while in the global method, the LAPACK [12] routine `dspev` is used for the diagonalization of the system of linear equations.

4. Detector description and alignment infrastructure

The description of the ATLAS detector is done in terms of basic geometrical primitives. These are grouped into the GeoModel toolkit, a set of libraries including both raw geometry and material information, and specific data of each ATLAS subsystem. The geometry is built from primary numbers which are stored in a relational database and logically grouped into a set of hierarchical nodes.

The alignment infrastructure within GeoModel is based upon alignable nodes which are updated from the Conditions Database by means of the Interval of Validity (IoV) service. As

Table 1. Misalignment levels within the Inner Detector. The reference frame for the corresponding transforms of each level is also quoted.

Level	Pixel	SCT	TRT	Reference frame
1	Whole detector	Barrel End-Caps	Barrel End-Cap	Global
2	Barrel layers End-Cap disks	Barrel layers End-Cap disks	Barrel modules	Global
3	Barrel modules End-Cap modules	Barrel modules End-Cap modules	-	Local

this mechanism is implemented at the detector description layer, the same infrastructure can be used for both simulation and reconstruction (independently or simultaneously).

The misalignments are introduced in terms of AlignableTransform objects, each of which contains a list of alignable transforms and associated identifiers. Each alignable transform is defined as a CLHEP HepTransform3D matrix, which contains the translation vector and rotation matrix of the object to be displaced.

Three different levels of misalignments exist for the Inner Detector (see table 1), although their meaning differ among each sub-system:

- **Level 1:** transforms represent movements of the main sub-detectors parts, like the SCT barrel, the two SCT end-caps, the TRT barrel and the two TRT end-caps. For the Pixel detector, no distinction is done for barrel and end-caps, so it is moved as a whole unit.
- **Level 2:** transforms represent movements of the silicon barrel layers, silicon end-cap disks and TRT barrel modules.
- **Level 3:** transforms represent movements of the silicon modules.

Individual module distortions or single straw misalignments are not implemented at the simulation level, but introduced at the reconstruction stage as additional displacements to the hit positions.

5. Validation of the alignment algorithms

The different alignment approaches have been extensively tested with simulated events and real data coming from the ATLAS Combined Testbeam and cosmic runs recorded in the surface assembly area. Some results are shown in what follows.

5.1. Combined Testbeam

The ATLAS Combined Testbeam (CTB) took place at CERN's H8 beamtest area during 2004. Detectors from all different ATLAS sub-systems were used in the final setup in order to reproduce a barrel slice of the ATLAS experiment starting from the interaction point at $\eta = 0$. The ID setup consisted in six pixel modules arranged in three layers, eight SCT modules in four layers and six TRT modules. Both the pixel and SCT detectors were located inside a magnet delivering a field up to 1.4 T, being the TRT outside. The distance between different layers and the overlap between modules within the same layer were chosen to be as close as possible to the modules arrangement in the barrel cylinders of the real experiment. A total number of 22 million events with all three ID subdetectors, including runs with different types of particles (e, π, μ and γ),

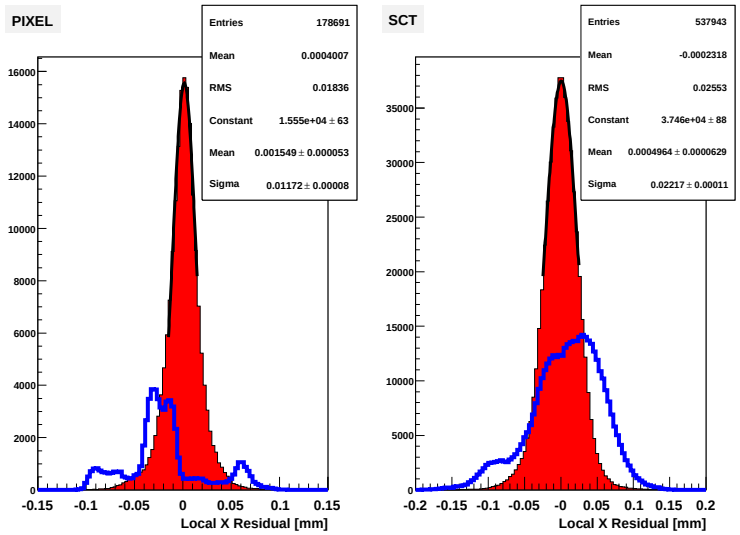

Figure 2. Pixel (left) and SCT (right) residuals in the most sensitive coordinate before (empty histogram) and after (filled histogram) alignment with the Robust approach on CTB real data.

energies (from 2 up to 180 GeV/c) and magnetic field configurations, were validated as usable for further offline analysis.

The different alignment algorithms were applied to a set of common reference runs of real data. The corrections derived by each of them were applied afterwards to reconstruct the trajectories of electrons and pions with magnetic field-on. Figure 2 shows a comparison of the Pixel and SCT residuals in their most precise coordinate before and after alignment as obtained with the Robust approach. The improvement with respect to the residuals of the modules located in their nominal positions is clear. A Gaussian fit to the final distributions leads to sigmas of $\sim 12\,\mu m$ and $\sim 22\,\mu m$ for Pixel and SCT respectively, being the mean centered around zero within a micron. For the whole period of runs analyzed, the precision reached in the alignment of the silicon modules is $\sim 5\,\mu m$ in their most precise coordinate [13].

Due to the particularities of the incoming beam distribution, typical in beamtest setups (almost all particles come parallel with almost perpendicular incidence on the detector planes), some degrees of freedom were not considered (*e.g.* displacements along the beam-axis). Some discrepancies were observed in the sets of alignment corrections provided by the different approaches. These were understood as global displacements of the whole setup. Track-based alignment algorithms remain almost insensitive to these global deformations (see section 6.3). The momentum measurement remains however as a powerful cross-check of the alignment. Figure 3 shows a comparison of the momentum resolution obtained with the local χ^2 approach for a 100 GeV π^+ pion run. Figure 4 shows $\sigma(p)/p$ as a function of the momentum for the different methods including simulation. An excellent agreement was found in all cases. The slightly worse momentum resolution obtained with the Robust approach is due to the limited number of DoFs considered in this case.

5.2. Cosmic data-taking

Cosmic-rays were recorded on the SR1 assembly area with the already assembled SCT and TRT barrels and with one of the two SCT and TRT end-caps. For the barrel test, two sectors of the SCT and TRT were cabled for readout, representing $\sim 22\%$ and $\sim 13\%$ of the entire SCT

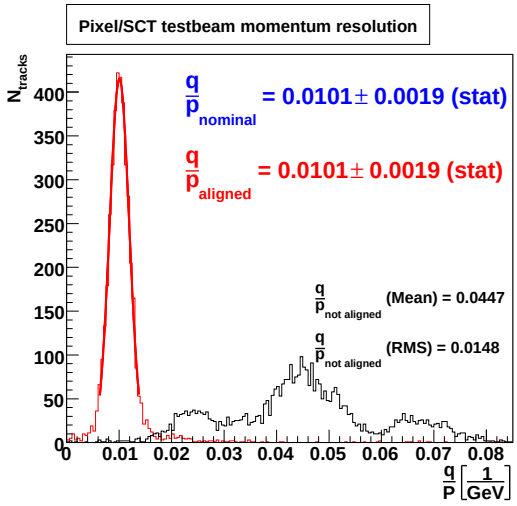

Figure 3. Momentum resolution of Pixel and SCT modules for a CTB run of 100 GeV π^+ without alignment corrections (non-fitted histogram) and with alignment corrections derived with the Local χ^2 method (Gaussian-fitted histogram).

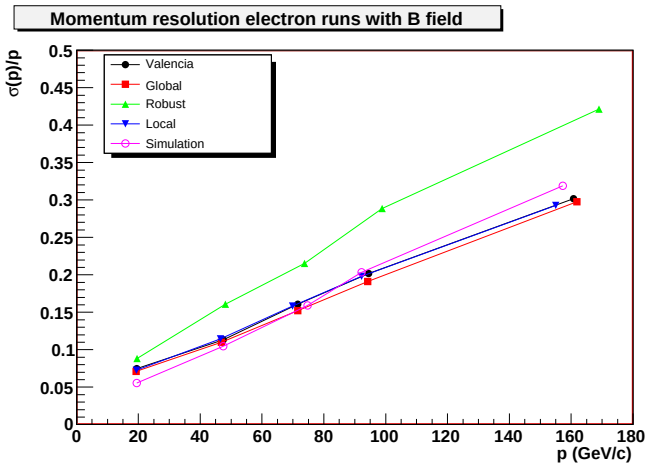

Figure 4. Comparison of the momentum resolution $\sigma(p)/p$ as a function of the momentum for CTB electron runs with B=1.4 T.

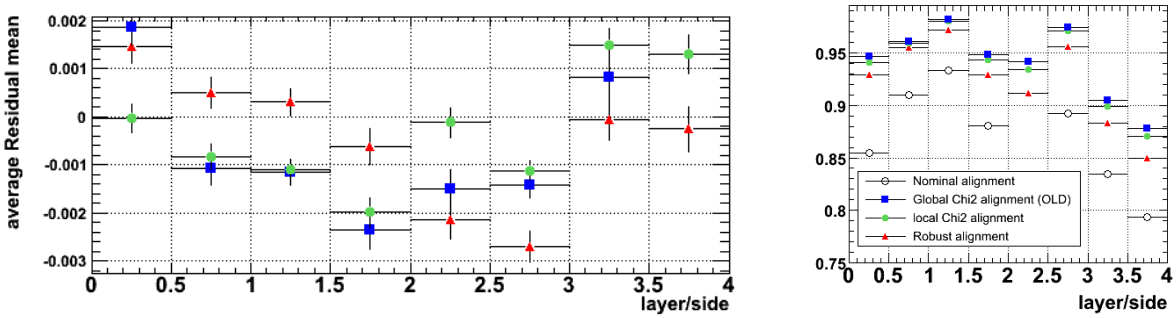

Figure 5. Average mean of SCT residuals (left) and SCT efficiency (right) as a function of layer and readout side after alignment of SR1 cosmic data with different alignment approaches. The results obtained with the nominal positions of the detectors correspond to open markers.

and TRT barrel detectors. The muon trigger was given by several scintillators on top of and below the setup placed according to the angular distribution of cosmic ray muons. Although a 15 cm thick concrete slab allowed to perform a momentum cutoff of $\sim$ 170 MeV, the data-taking was performed without magnetic field, implying MCS effects from low momentum tracks in the different alignment procedures.

Figure 5 shows the average mean of the SCT residual distributions as a function of the layer number and readout side for different alignment algorithms. Shifts of the order of $\sim 100\,\mu m$ in the most sensitive coordinate were found, in accordance from the expectations from the built tolerances. The overall residual means are constrained within a $\sim 5\,\mu m$ window. After alignment, the hit efficiency is increased, as can be seen in the right plot from figure 5.

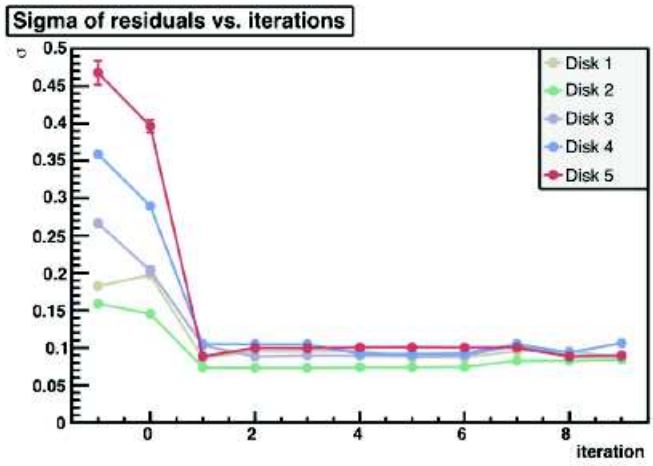

Figure 6. Sigma of the Gaussian fit to the residual distributions (SR1 cosmic data) for the first five SCT end-cap disks as a function of the iteration number.

The benefits of coupling the survey information with the track-based alignment procedures is well illustrated in figure 6, which shows the sigma of a Gaussian fit to the residual distributions for the first five SCT end-cap disks as a function of the iteration number obtained with the global method of TRTAlignAlg. Iteration labeled as "-1" corresponds to the nominal positions of the end-cap disks. In iteration "0", the information from the survey measurements is taken into account, resulting in a significant decrease of the residual widths. Stable results are obtained just after performing a single alignment iteration.

6. Computing System Commissioning and Calibration Data Challenge

6.1. Introduction

The *Computing System Commissioning* (CSC) and *Calibration Data Challenge* (CDC) are intended to exercise the full ATLAS software chain before the start of data-taking. The aim is to validate all aspects of the computing model, from generators to physics analysis, by defining specific sub-systems tests with well defined goals. Among these, an important aspect is to test the alignment and calibration algorithms with an imperfect (realistic) detector description of the ATLAS experiment.

Specifically for the Inner Detector, the *as-built* geometry includes misalignments of the different sub-systems, distorted material and distorted (tilted and shifted) magnetic field [14]. The misalignments range from $\mathcal{O}(1\,\mathrm{mm})$ and $\mathcal{O}(0.1\,\mathrm{mrad})$ for level 1 translations and rotations respectively, to $\mathcal{O}(100\,\mu m)$ and $\mathcal{O}(1\,\mathrm{mrad})$ for levels 2 and 3. The effect of the detector misalignments is shown in figure 7, where the mass resolution of the muon pair from $Z \rightarrow \mu\mu$ decays is shown, as using only the Inner Detector for event reconstruction.

The exercise is foreseen to be a *closed-loop*, where the alignment and calibration corrections will be computed after the reconstruction on a miscalibrated and misaligned simulated detector. Starting with a blind knowledge of the constants, a first set of calibration and alignment parameters is derived and then applied in a subsequent data reconstruction. A new set of constants is then determined and the process repeated again. The performance of the detector (track parameters, fit quality, residual distributions, etc.) is expected to improve in successive reconstruction passes.

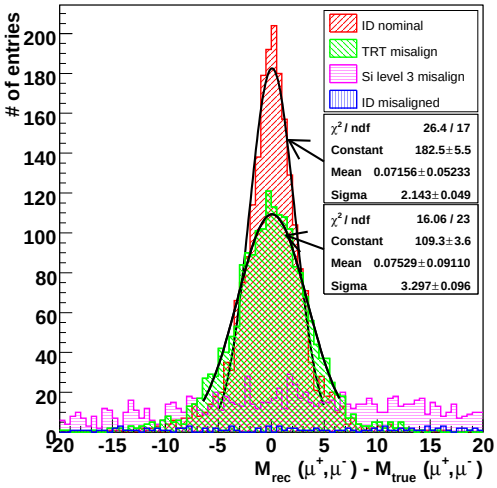

Figure 7. Mass resolution of the muon pair from $Z \rightarrow \mu\mu$ decays after event reconstruction with the whole Inner Detector (*as-built* geometry).

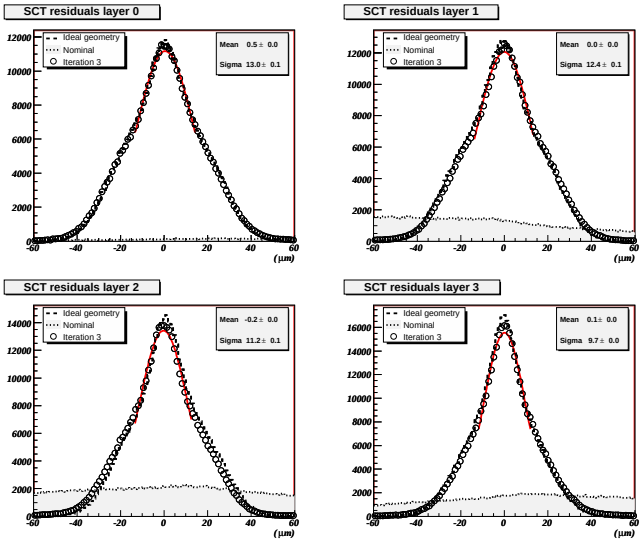

Figure 8. SCT residuals per barrel layer. Results with the filled histograms, – – – and ○○○ curves correspond respectively to the *as-built* geometry, ideal geometry and after alignment.

6.2. Simulated sample

For the Inner Detector alignment community, a multimuon sample with 10^5 events has been simulated with the realistic detector description. The multiplicity is 10 muons per event (alternating charge in consecutive events), all of them generated from the same point and uniformly distributed in η and ϕ. The primary vertex has been generated from Gaussian distributions of widths $15\,\mu m$ and $56\,mm$ respectively in the transverse plane and along the beam-axis. The transverse momentum spectrum range is [2;50] GeV/c. Figure 8 shows the SCT residuals per barrel layer after three iterations with the Global χ^2 alignment algorithm. The results are in very good agreement with what is expected from the ideal ID geometry.

6.3. Sagitta distortions

Correct residual distributions are required but not enough to guarantee a proper alignment. Sagitta distortions correspond to detector distortions which systematically bias some of the track parameters while keeping a general helical path. A schematic example is shown in figure 9, where a translation along the X-axis (in the plane transverse to the beam-axis) of the silicon barrel layers of an amount proportional to their radius squared produce a bias in the transverse momentum. These kind of global deformations are hardly detected by any alignment algorithm based on residuals minimization. As can be seen from the correlation plot in figure 10, after performing an alignment only at the module level (level 3), the transverse momentum distribution is biased. An alignment of the support-structures (levels 1 and 2) remains thus mandatory to recover the track parameters.

6.4. Sagitta removal

Several methods exist to remove (or at least, to keep under control as much as possible) the sagitta distortions. These include for example the usage of different event topologies (cosmic muons, beam-gas interactions, J/Ψ and Z decays, etc.), redundant measurements within the

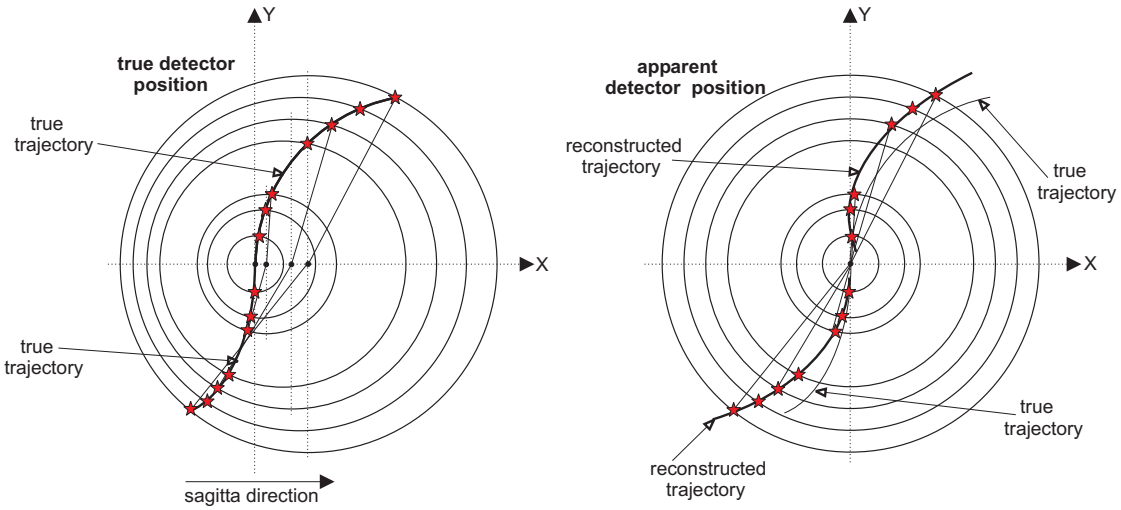

Figure 9. Transverse momentum bias due to a sagitta along the X-axis consisting in a translation proportional to r^2, being r the radius of each silicon barrel layer.

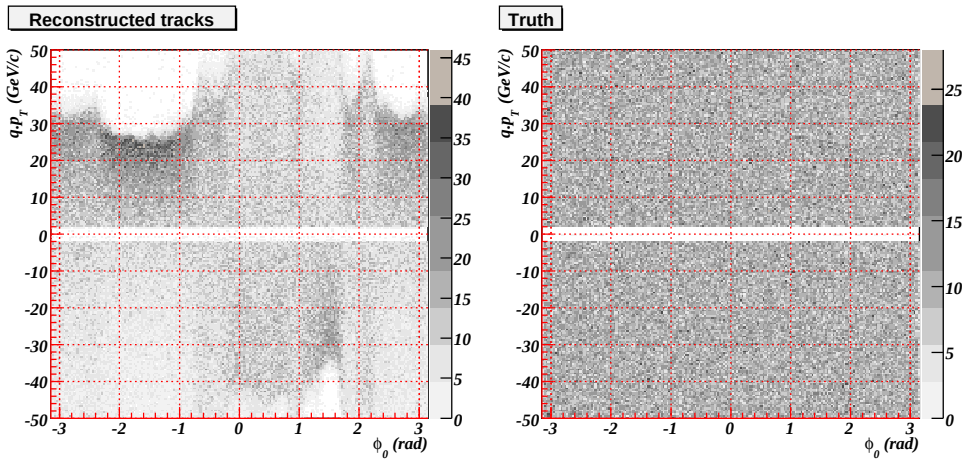

Figure 10. Signed p_T as a function of the track azimuthal angle ϕ_0 after an alignment performed just at the module level (left) and truth values (right).

same experiment (momentum measurement in the Muon Spectrometer), external constraints (survey measurements, FSI system, etc.), energy-momentum relation from the calorimeters, etc.

For the Inner Detector, one can make use of a simple offline analysis to remove some of the global deformations. Due to entire subdetector movements, the position of the primary vertex or beamspot may appear to be artificially shifted, originating a dependence of the transverse impact parameter d_0 with respect to the azimuthal angle ϕ_0 of the reconstructed tracks. This is shown in figure 11. A fit to the correlation plot leads to the displacements $x_0 = (-0.655 \pm 0.005)$ mm and $y_0 = (-1.045 \pm 0.004)$ mm, to be compared with the displacement of the entire Pixel detector in the transverse plane (level 1) of $x_{\mathrm{Pixel}} = 0.60$ mm and $y_{\mathrm{Pixel}} = 1.05$ mm. As expected, the resolution in the transverse impact parameter is mostly determined by the innermost silicon layers. Another example is shown in figure 12, where the benefits of combining different event samples (multimuons and cosmics in this case) in the alignment procedure is obvious. The transverse momentum asymmetry is almost completely recovered.

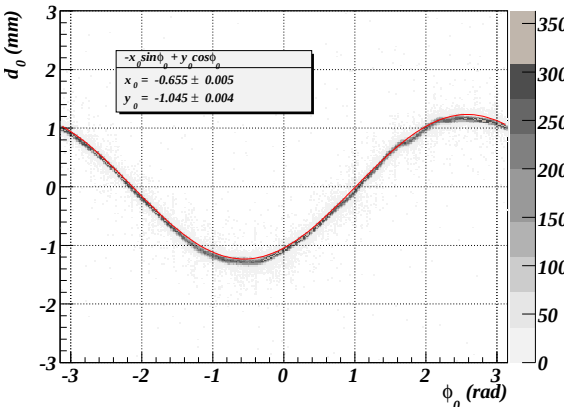

Figure 11. Correlation between d_0 and ϕ_0 for reconstructed tracks.

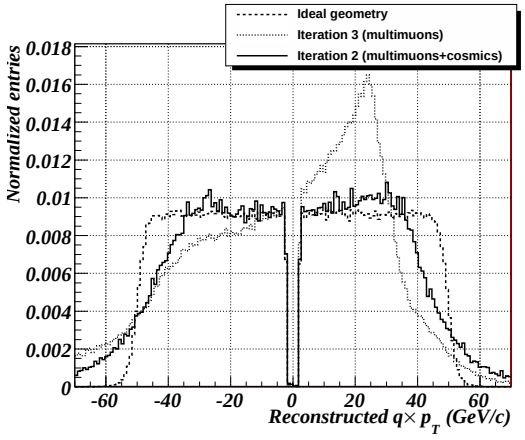

Figure 12. Comparison between the signed transverse momentum distribution obtained only with the CSC multimuon sample and after combining it with cosmic events. Results from the ideal geometry are also included.

7. Summary

Several track-based alignment algorithms have been developed for the alignment of the ATLAS Inner Detector. Already validated with real data from the ATLAS Combined Testbeam and cosmic muon runs, work is pursued in a final stage where a realistic detector description has been implemented at the simulation level. The understanding of systematics (sagitta distortions) remains crucial to achieve the ultimate precisions required.

Acknowledgments

The author is grateful to the whole ATLAS alignment and tracking groups for useful discussions.

References

[1] ATLAS Technical Proposal, CERN/LHCC/94-43 (1994).
[2] ATLAS Inner Detector Technical Design Report, CERN/LHCC97-16 & CERN/LHCC97-17 (1997).
[3] Gianotti, F. "Precision Physics at the LHC". ATL-PHYS-99-001.
[4] Heinemann, F. "Track based alignment of the ATLAS silicon detectors with the Robust alignment algorithm". ATL-COM-INDET-2007-014 (2007).
[5] Brückman de Renstrom, P. et al. "Global χ^2 approach to the alignment of the ATLAS silicon tracking system". ATL-INDET-PUB-2005-002 (2005).
[6] Hicheur, A. et al. "Implementation of a global fit method for the alignment of the silicon tracker in the ATLAS Athena framework". CHEP06 Proceedings, Mumbai (India) (2006).
[7] Morley, A. "Alignment of the ATLAS silicon tracker". FD07 Proceedings, (2007).
[8] Härtel, R. "Iterative local Chi2 alignment approach for the ATLAS SCT detector". Master thesis (2005).
[9] Goettfert, T. "Iterative local Chi2 alignment approach for the ATLAS Pixel detector". Master thesis (2006).
[10] Bocci, A. et al. "TRT Alignment for SR1 cosmics and beyond". ATL-INDET-PUB-2007-009 (2007).
[11] CLHEP - A class library for high energy physics. `http://proj-clhep.web.cern.ch/proj-clhep/`.
[12] LAPACK - Linear Algebra PACKage. `http://www.netlib.org/lapack/`.
[13] Gonzalez-Sevilla, S. et al. "Alignment of the Pixel and SCT Modules for the 2004 ATLAS Combined Test Beam". ATL-COM-INDET-2007-013 (2007).
[14] Ahmad, A. et al. "Inner Detector as-built detector description validation for CSC". ATL-INDET-INT-2007-002. (2007)
[15] Blusk, S. et al. "Proceedings of the first LHC Detector Alignment Workshop". CERN Yellow Book 2007-004. (2007)